

The Time Development of a Blast Wave
with Shock Heated Electrons

NASA-CR. 177888

Richard J. Edgar

and

Donald P. Cox¹

Space Physics Laboratory, Department of Physics
University of Wisconsin-Madison

Received _____

Abstract

Accurate approximations are presented for the time development of both edge conditions and internal structures of a blast wave with shock heated electrons, and equal ion and electron temperatures at the shock. The cases considered evolve in cavities with power law ambient densities (including the uniform ambient density case) and have negligible external pressure. Account is taken of possible saturation of the thermal conduction flux. The structures evolve smoothly from those given by Cox and Edgar (1981) to the adiabatic structures given by Cox and Franco (1981).

¹Also, Department of Space Physics and Astronomy, Rice University

This work continues a project begun in Cox and Edgar (1983, hereafter Paper I), modelling spherically symmetric supernova blast waves in a power-law ambient density distribution. The gas is assumed to be ideal, totally ionized, and the helium abundance is 10% of the hydrogen abundance by number. We have assumed also that non-coulomb processes heat the electrons in the shock, so that the electron and ion temperatures are equal immediately behind the shock. Thermal conduction is then important at early times when the temperature is high, but less important later, when the electron temperature and conductivity are lower. Our formulation of the thermal conduction flux follows that of Cowie (1977), which accounts for saturation effects.

We report here an approximate solution to the evolution of temperature, density, and pressure structures of such a supernova remnant. We separate, via physically reasonable approximations, the immediate postshock behavior from the evolution of the system as a whole, and solve for the evolution of the postshock conditions. We then separate, again by reasonable approximations, the dynamical and thermal evolution of individual gas parcels from that of the overall structure, and follow conditions in these parcels. Knowledge of the history of each parcel would facilitate the calculation of ionization fractions, which may be far from equilibrium.

We thus continue a study of the first order effects of thermal conduction on the structure, spectrum, and surface brightness distribution of a "non-radiative" remnant, including as much physics as possible, while avoiding the numerical solution of coupled partial differential equations.

The notation for the variables we have used is listed in Table 1, along with that of their post-shock derivatives ($\partial \ln f / \partial \ln R$) and normalized forms. As in Paper I, the jump conditions and their derivatives are given by

$$p_s = \rho_0 v_s^2 \left(\frac{x_s^{-1}}{x_s} \right),$$

$$\frac{F_s}{\rho_0 v_s^3} = \frac{x_s^{-1}}{2x_s^2} (4 - x_s), \quad (1)$$

$$u_s = \frac{x_s^{-1}}{x_s} v_s,$$

and

$$v_s^* = \frac{1}{2} \left(\omega - 3 - \frac{x_s^*}{x_s - 1} \right),$$

$$u_s^* = \frac{1}{2} \left(\omega - 3 + \frac{x_s^*}{x_s - 1} \right), \quad (2)$$

$$\rho_s^* = x_s^* - \omega,$$

where $\rho \propto R^{-\omega}$ was assumed for the ambient density, the asterisk represents the logarithmic derivative $f_s^* \equiv \partial \ln f_s / \partial \ln R_s$, F_s is the thermal conduction flux just inside the shock, and v_s is the shock velocity. In addition, ambient pressure has been neglected, and $p_s^* = -3$ has been assumed. This last is equivalent to assuming $p_s R_s^3$ is

constant, which cannot be exactly correct, but reflects the general effect of conservation of energy. In Paper I it was shown that the early and late asymptotes have $p_s R_s^3$ which differ by only a few percent at most (depending on ω). This assumption may tend to smooth over real short term excursions in pressure but prevents spurious approximation-induced variations and thus provides a physically based stability to the behavior.

Writing the post-shock equations of motion for a gas parcel in terms of the logarithmic derivatives given in Table 1 produces several relations among these quantities. Mass and momentum conservation give

$$\beta = \frac{\alpha}{x_s - 1} - \frac{3}{2} \frac{x_s x_s^*}{x_s - 1} + \frac{3}{2} x_s - 2 - \omega x_s \left[\frac{1}{2} - \frac{1}{x_s - 1} \right] \quad (3)$$

$$\frac{4 - x_s}{3} \left(\frac{R_s \ell_s}{F_s} \right) = \left(\beta - \frac{5}{3} \alpha \right) + x_s \left(3 + \frac{5}{3} x_s^* - \frac{5}{3} \omega \right).$$

The energy equations for the ions and electrons can be separated (Paper I) and written in the form

$$\frac{D}{Dt} \left(\frac{T^{3/2}}{n} \right) = - \left(\frac{T^{3/2}}{n} \right) \frac{\ell}{p} \quad (4)$$

$$\frac{D}{Dt} \left\{ \frac{[(\frac{2.3}{1.2} - g)T]^{3/2}}{n} \right\} = -a \left(\frac{2.3}{1.2} \right) \left(\frac{2.3}{1.2} - g \right)^{1/2} \frac{(1-g)}{g^{3/2}}, \quad (5)$$

where $T = (1.1T_i + 1.2T_e)/2.3$ is the average temperature, $g = T_e/T$, and $\ell = (1/R^2)(\partial/\partial R)(R^2 F)$ is the divergence of the thermal conduction flux. We have assumed here that $T_e \gg T_i/2000$. The constant

$a \approx \ln \Lambda / 153$ cgs where $\ln \Lambda = \ln[1.2 \times 10^5 (T_e^{1/2} / n^{1/2})]$. Also, $n = n_H + n_{He} = 1.1n_H$, $p_i = nkT_i$, $p_e = (1.2/1.1)nkT_e$, so that the ideal gas law becomes $p = (2.3/1.1)nkT$.

Equation (5) can be solved at $R = R_s$ (using the assumed $g_s=1$ appropriate to electron and ion temperature equilibration by non-coulomb processes in the shock) for $v \equiv (\partial \ln g / \partial \ln R)_s$ to produce

$$v = \frac{1.1}{1.2} \frac{4-x_s}{3} \left(\frac{R_s \ell_s}{F_s} \right). \quad (6)$$

Writing equation (4) in terms of $\eta \equiv -(\partial \ln T_e / \partial \ln R)_s$ and making use of the fact that $-\eta = v + (\beta - \alpha)$, it follows that

$$(5x_s - 8)(\eta + v) = (6x_s^2 - 11x_s - 4) - \omega x_s(4x_s - 7) + x_s x_s^*(5x_s - 7) - (x_s - 2)(4 - x_s) \frac{R_s \ell_s}{F_s}, \quad (7)$$

which, together with equation (6) gives us η as a function of x_s , x_s^* , and $R_s \ell_s / F_s$.

To evaluate the thermal conduction flux, we use the form given by Cowie (1977) for the ratio of true flux to classical (i.e. non-saturated) flux:

$$\frac{F}{F_c} = \frac{1}{1 + \frac{4.6 \eta \lambda}{\phi_s R_s}}, \quad (8)$$

where ϕ_s is a plasma parameter of order unity (we have used $\phi_s = 1$ throughout), and λ is the mean free path for electron energy exchange.

In our case, for conditions just inside the shock front, the second term in the denominator can be written (using $\lambda = m_e^{1/2} b T^2 / (1.31 n_e k^{3/2})$ where $b \approx 6 \times 10^{-7}$ (30/ln Λ) cgs, from Cowie and McKee (1977), the jump conditions relating F_s , v_s , $\rho_0 v_s^3$, p_s , and the ideal gas law)

$$\frac{4.6 \eta \lambda}{\phi_s R_s} = \frac{1}{10 \phi_s} \frac{4-x_s}{(x_s-1)^{1/2}} \frac{F_c}{F}, \quad (9)$$

whence it follows that

$$\left(\frac{F}{F_c} \right)_s = 1 - \frac{1}{10 \phi_s} \frac{4-x_s}{(x_s-1)^{1/2}}. \quad (10)$$

Notice that the degree of saturation of the thermal conduction flux just behind the shock is simply related to x_s . The conduction is never heavily saturated and becomes classical as x_s approaches 4. The classical flux at R_s can be written

$$\left(\frac{F}{F_c} \right)_s = -b T_e^{5/2} \left(\frac{\partial T_e}{\partial R} \right)_s = \frac{b T_s^{7/2}}{R_s} \eta. \quad (11)$$

Hence

$$\eta = \frac{R_s F_s}{b T_s^{7/2} \left[1 - \frac{1}{10 \phi_s} \frac{4-x_s}{(x_s-1)^{1/2}} \right]}. \quad (12)$$

In this equation, T_s and F_s can be eliminated using equation (1) and the ideal gas law. The result can be written

$$\eta = \frac{x_s^3 (4-x_s)}{(x_s-1)^{1/2}} \frac{z^{7-3\omega}}{\left[1 - \frac{1}{10 \phi_s} \frac{(4-x_s)}{(x_s-1)^{1/2}} \right]}, \quad (13)$$

where z is a normalized radius defined by

$$z^{7-3\omega} = \left(\frac{R_s}{R_1} \right)^{7-3\omega} = \frac{1}{2m^{1/2}} \left[\frac{2.3}{1.1} k \right]^{7/2} \frac{R_s n_0^3}{b p_s^2}. \quad (14)$$

The $z^{7-3\omega}$ dependence follows from $n_0 \propto R_s^{-\omega}$ and $p_s \propto R_s^{-3}$. In this formula, $m = \rho/n = (1.4/1.1)m_H$. The formula for determining the constant R_1 depends on energy integrals which we shall discuss later.

From equation (13), it is clear that η depends very sensitively on R_s in the vicinity of R_1 . For small values of z , η will be extremely small and the electron temperature will be flat. For large values of z , however, x_s is driven to 4 to keep η from becoming very large. In fact, η approaches $4-3\omega$ in the adiabatic limit.

In order to reduce the evaluation of the dynamics of this blast wave to the solution of ordinary differential equations, one further piece of information is required, namely the behavior of the parameter

$R_s \ell_s / F_s$. This parameter was discussed at some length in Paper I for the early time asymptote. In particular we can write

$$\frac{F_s}{R_s} = \frac{1}{0} \int_0^1 r^2 \ell dr = \int_0^1 r^2 x \left(\frac{\ell}{x} \right) dr = \left\langle \frac{\ell}{x} \right\rangle \frac{1}{3-\omega}, \quad (15)$$

where $\langle \ell/x \rangle$ is the mass average of the energy loss rate per n_0 particles due to conduction. If all electrons lose energy at approximately equal rates via this mechanism, then $\langle \ell/x \rangle \sim \ell_s/x_s$ and $\ell_s R_s / F_s = x_s(3-\omega)$. It was found in Paper I that in fact ℓ/x varies very little over the structure of the young blast wave (see figures 1b, 2b, and 3b of Paper I) and that $R_s \ell_s / F_s \approx x_s(2.53-\omega)$ fit the edge results very well. This is certainly the value we need at the beginning of our evolution, but we are about to argue that it is probably an adequate approximation throughout.

At late times (z just slightly greater than 1 constitutes late times) x_s is driven to 4 as we have seen. Since $R_s \ell_s / F_s$ is everywhere in the equation multiplied by $(4-x_s)$, the particular form of $R_s \ell_s / F_s$ is unimportant. Thermal conduction simply fades away.

During the transition period, however, there is a very complex set of interactions. Thermal conduction is suddenly finite, allowing significant gradients in T_e to develop behind the shock. At the same time (e.g. Cox and Anderson, 1982, hereafter CA), coulomb heating is becoming important near the edge. The coulomb heating is proportional to $T_i - T_e$, however. If thermal conduction is truly insignificant, T_e will remain at T_i behind the shock and coulomb heating will do nothing. If thermal conduction is still important, T_e will fall just

far enough below T_i that coulomb heating can supply the losses. Thus a competition develops between two processes for control of the gradient in T_e . At some moment, control will pass decisively to coulomb heating, and the difference between T_e and T_i will become imperceptible over a progressively larger region. This kind of behavior is shown in both CA and Cox and Franco (1981, CF) for blast waves with coulomb heating only.

Because of the sensitivity of both coulomb heating and thermal conduction to the post shock gradient of T_e as one enters the transition, the conduction flux and $T_i - T_e$ will be difficult to approximate reliably from first principles. The ratio ℓ_s/F_s , however, can be expected to vary rather smoothly. Apart from a very short lived transient during which near equilibration has been achieved only at the immediate edge, the ratio should never be very far from the mass average. (The mass is far too heavily concentrated near the edge for the result to be otherwise.) In short, approximating $R_s \ell_s/F_s$ throughout by $x_s(2.53-\omega)$ may provide a very slight smoothing of the behavior near the onset of the rapid transition, but as a rule it should be very nearly correct; it makes no a priori judgement about the magnitudes of F_s or ℓ_s ; it is exact at early times when thermal conduction is most important; and it does not interfere with the approach to negligibility of thermal conduction at late times.

With this approximation, equations (6) and (7) combine to produce an ordinary differential equation $x_s^*(z, x_s)$:

$$x_s^* = \frac{z}{x_s} \frac{dx_s}{dz} = \frac{1}{x_s(5x_s-7)} \{ (5x_s-8) \left[\eta + \frac{1.1}{1.2} \frac{4-x_s}{3} x_s(2.53-\omega) \right] \quad (16)$$

$$- (6x_s^2-11x_s-4) + \omega x_s(4x_s-7) + (x_s-2)(4-x_s)x_s(2.53-\omega) \}$$

with η given in (13).

The initial conditions for this equation are provided by Paper I. In the early time (small z) limit, $x_s^* \approx 0$, and the η term can be neglected (thus reducing equation (16) above to equation (17) of Paper I), so that the solutions for the compression factor $x_s(\omega)$ given in Table 1 of Paper I can be adopted as initial values.

It should be noted here that the Paper I results for $x_s(\omega)$ and that $(R_s \ell_s / F_s) \approx (2.53-\omega)x_s$ follow from the assumption that the interior density structure is approximately that given by Kahn (1975) as generalized by CA. This approximation (which automatically conserves mass) was tested against analytic results for adiabatic blast waves by CF and found to be accurate to within a few percent (and much closer near the edge where the mass is concentrated).

We have found solutions to equation (16) by numerical integration for $\omega = 0, -2$, and -4 (uniform density and cavities of various steepness). The integration provides x_s and x_s^* as functions of z , and introducing these into the post-shock derivative equations supplies α , β , v , and η all as functions of z . When the results are combined with the jump conditions and ideal gas law, they completely specify the immediate post-shock values of p_s , n_s , T , and T_e and their spatial derivatives. The results are shown in Figure 1. A good approximate method for generating these functions for application to a particular

problem is presented in section III. A few properties of these solutions are given in Table 2.

Shock radius as a function of time follows from the first jump condition in equation (1):

$$p_s = \rho_0 v_s^2 \frac{x_s^{-1}}{x_s} = \frac{2}{3\epsilon(\omega)} \frac{E_0}{\frac{4}{3}\pi R_s^3} \quad (17)$$

where $\epsilon(\omega) = 2E_0/3V_s p_s$ is the energy integral given in Paper I, and repeated in Table 2 for reference. Here V_s is the volume of the remnant. Defining a natural time unit of

$$t_1 = \left[\frac{2\pi \epsilon(\omega) \rho_0 (R_1) R_1^5}{E_0} \right]^{1/2}, \quad (18)$$

we obtain the ordinary differential equation

$$\frac{d\tau}{dz} = \left[\frac{x_s^{-1}}{x_s} z^{3-\omega} \right]^{1/2} \quad (19)$$

for the age of the remnant $\tau \equiv t/t_1$ as a function of shock radius $z \equiv R_s/R_1$. Numerical integration is straightforward. The results are well approximated by a power law $\tau \propto z^{(5-\omega)/2}$, the maximum discrepancy amounting to about 3%. Figure 2 shows the behavior predicted by this integration.

II. The Interior Structure

In this section we will derive the approximate internal density, pressure, and temperature structures of the remnant. The approach we will follow is to solve the equations of motion for selected gas parcels from the time they are shocked as they move into the interior of the remnant.

A convenient coordinate to use in tracking gas parcels is the mass fraction $\mu \equiv M(R)/M$, where $M(R)$ is the mass enclosed within a radius R (which is constant for a given gas parcel, though R changes) and M is the total mass of the remnant, which increases as the shock encompasses more material.

The density structure will be assumed (as above) to be given by the approximation of Kahn (1975) as generalized by CA:

$$x = \left[\frac{5}{2} + (x_s - \frac{5}{2})r^q \right] \frac{\mu(r)}{r^3},$$

$$\mu(r) = \{r^{5/2} \exp[(x_s - \frac{5}{2})\frac{r^q - 1}{q}]\}^{3-\omega} \quad (20)$$

$$q = \frac{x_s(3+\alpha) - (3-\omega)x_s^2}{x_s - \frac{5}{2}}.$$

The approximation conserves mass, provides the correct density and slope at R_s , and the correct logarithmic slope at $R \ll R_s$.

For a given gas parcel i which was shocked at z_i , we can calculate its present radius $r \equiv R/R_s$ by noting that $\mu_i = (z_i/z)^{3-\omega}$ (since $M(R)$ has increased in proportion to $z^{3-\omega}$), and solving the

second of equation (20) numerically for r . Using (20) we then have the local density, since $n = x n_0(z=1) z^{-\omega}$.

To find the remaining quantities of interest (p , T , and T_e), we need two equations (plus the ideal gas law). These equations are provided by equations (4) and (5) above. It is convenient to choose as variables the "adiabatic constant" K , conveniently normalized, and another quantity C :

$$K \equiv \frac{1}{A} \frac{T^{3/2}}{n}, \quad (21)$$

$$C \equiv \left[\frac{2.3}{1.2} - g \right]^{3/2} K,$$

$$A \equiv \frac{1.4}{1.1} \left(\frac{1.4}{2.3} \right)^{3/8} \frac{m_H^{5/2}}{k^{3/2}} \left\{ \frac{p_s(z=1)}{[\rho_0(z=1)]^{5/3}} \right\}^{3/2},$$

where m_H is the mass of a hydrogen atom and $g = T_e/T$ as before. The normalization constant A is chosen so that the initial value of K is particularly simple in form; see below. Then using the first 2 members of equation (1), equation (6), and replacing time derivatives with z derivatives using $z(D/Dz) = (R_s/v_s)(D/Dt)$ we can rewrite equations (4) and (5) in the more convenient form

$$\frac{DK}{Dz} = - \frac{K}{z} \left[\frac{3}{2} \frac{x}{x_s^2} \cdot \frac{12}{11} \cdot \frac{v}{y} x(\mu) \right], \quad (22)$$

and

$$\frac{DC}{Dz} = -G \left(\frac{2.3}{1.2} - g \right)^{1/2} \frac{(1-g)}{g^{3/2}} z^{\frac{3-\omega}{2}} \left(\frac{x_s-1}{x_s} \right)^{1/2} \quad (23)$$

where $y = p/p_s = (x/x_s)^{5/3} (K/K_s)^{2/3}$, $G = \frac{a}{A} \left(\frac{2.3}{1.2} \right) t_1 = 11.37$, and $\chi(\mu) \equiv (\ell/\rho)/(\ell_s/\rho_s)$ is the normalized divergence of the thermal conduction flux.

Using equation (16) from Paper I and the approximation discussed above that $R_s \ell_s / F_s \approx x_s (2.53 - \omega)$, a bit of algebra produces the result

$$\chi(\mu) = \frac{1.2}{2.3(2.53-\omega)(4-x_s)} \left(9 - 5\omega - \frac{2}{r^2} \frac{x'}{x^2} \mu \right), \quad (24)$$

where $x' = \partial x / \partial r$ and r is given in terms of μ by inverting equations (20). This formula was derived assuming self-similarity, and is therefore only valid at early times (the situation addressed in Paper I). We will take the same functional form for $\chi(\mu)$ at all times, which necessitates using early-time asymptotic values for x_s and q in equation (24) and the supporting equations (20). Thus at early times when the thermal conductivity is large it is correctly accounted for, and while the approximation is less accurate at later times, the right-hand side of equation (22) is approaching zero since $v \propto (4-x_s)$. Thus the approach to the final adiabatic ($K \propto T^{3/2/n} = \text{constant}$) condition is preserved, though the rate of approach may not be correct.

We now have a pair of coupled equations, which can be solved subject to the initial conditions (i.e. post-shock values) derived above, rewritten in the form

$$K_s = [x_s(z)]^{-5/2} z^{\left(\frac{5\omega-9}{2}\right)}$$

$$C_s = \left[\frac{2.3}{1.2} - 1\right]^{3/2} K_s. \quad (25)$$

The solutions to these equations for representative parcels has been carried out, and snapshots of the resulting structure are presented in Figures 3, 4, and 5. The density plots are normalized to $\rho_0(z=1)$ or $n_0(z=1)$, the pre-shock density at $R_s=R_1$. The temperature and pressure graphs are plotted in units of the post-shock values at $R_s=R_1$:

$$T_s(z=1) = 1.03 \times 10^7 \text{ K} \left(\frac{E_{51}}{\epsilon(\omega)}\right) \frac{1}{x_s(z=1)n_0(z=1)} \left(\frac{12.2 \text{ pc}}{R_1}\right)^3 \quad (26)$$

$$p_s(z=1) = 2.97 \times 10^{-9} \text{ dyne cm}^{-2} \left(\frac{E_{51}}{\epsilon(\omega)}\right) \left(\frac{12.2 \text{ pc}}{R_1}\right)^3,$$

where $\epsilon(\omega)$ is the energy integral from table 2, E_{51} is the explosion energy E_0 in units of 10^{51} ergs, and R_1 can be calculated from equation (27) below.

The reader will notice the small waves near the edges of the last snapshots in the temperature and pressure plots given in Figures 3-5. We expect the sudden transition to introduce such waves, but the particular form shown is probably rather heavily influenced by our approximation scheme, in particular the constraints of the density structure to the Kahnian form and the post shock pressure to R_s^{-3} development. Considering that the model was probably forced to evolve somewhat more smoothly than the actual transition, the wave amplitudes should probably be regarded as a lower limit to both the uncertainty on local conditions and the expected transient amplitudes.

III. Application of These Results

In general one wishes to calculate the conditions in a remnant with some particular explosion energy, E_0 , shock radius R_s , and pre-shock density $\rho_0(R_s) \propto R_s^{-\omega}$ and one is hopefully content with one of the values $\omega = 0, -2$, or -4 . If one wishes to assume that there is no non-coulomb heating in the shock or no thermal conduction, one turns directly to CF. If one wishes to include a significant external pressure, is content with $\omega=0$, and either no non-coulomb heating or no thermal conduction, one turns to CA. Those two papers are also useful if one is interested in an epoch significantly later than the electron equilibration time (discussed in either paper). If one is interested in a case with non-coulomb heating ($T_e = T_i$ at the shock) and strong thermal conduction for times much less than the equilibration time, one turns to Paper I. Only if one is forced to be interested in the structure of a remnant with non-coulomb heating and thermal conduction

in the vicinity of the equilibration epoch will one wish to follow the procedure below.

For given values of E_0 , R_s , $\rho_0(R_s)$ and ω , one first finds $\epsilon(\omega)=2E_0/3V_s p_s$ from Table 2. One can choose a value for the early asymptote, the late asymptote, or somewhere in between, depending on whether the time of interest is relatively early, late, or intermediate in the transition. (The values are very similar and one should worry very little over the choice.) From this choice, one can then calculate p_s . The mean mass per nucleus is $m=1.4m_H/1.1$ and $n_0=\rho_0/m$.

The radius and time units R_1 and t_1 can then be calculated from

$$R_1 = 12.2 \text{ pc} \left\{ \left(\frac{R_s}{12.2 \text{ pc}} \right)^{-3\omega} \left(\frac{E_{51}}{\epsilon(\omega)} \right)^2 \frac{30}{\ln \Lambda} [n_0(R_s)]^{-3} \right\}^{\frac{1}{7-3\omega}} \quad (27)$$

$$t_1 = 3.19 \times 10^4 \text{ y} \left\{ \left(\frac{R_s}{12.2 \text{ pc}} \right)^{-4\omega} \left(\frac{E_{51}}{\epsilon(\omega)} \right)^{\frac{3+\omega}{2}} \left(\frac{30}{\ln \Lambda} \right)^{\frac{5-\omega}{2}} [n_0(R_s)]^{-4} \right\}^{\frac{1}{7-3\omega}}$$

which follow from equations (14), (17), (18), the ideal gas law, and the fact that $n_0(R_s) \propto R_s^{-\omega}$. The present maturity of the shock is then $z_p = R_s/R_1$, and the age of the shock can be read from Figure 2. The postshock temperature and pressure and the preshock density at $z = 1$ (which are the units of the ordinates in Figures 3-5) can then be found from

$$\rho_0(R_1) = \rho_0(R_s) \left(\frac{R_s}{R_1}\right)^{-\omega} \quad (28)$$

and equations (26).

If one is interested in only a cursory picture of the remnant state, the postshock compression can be read from the appropriate figure. The shock velocity, postshock mass velocity, and thermal conduction flux are found from equation (1) and the postshock temperature (and electron temperature since $T_e = T$ was assumed at the shock) from $T = 1.1 p / (2.3 nk)$. The logarithmic derivatives of ρ , p , T , T_e , and T_e/T , can all be read from the graphs. If z_p is close to one of the those represented in Figure 3, the remainder of the normalized structure is shown.

If, however, one requires a rigorous numerical description in order, for example, to calculate the past evolution to R_s and the ionic concentrations now present, this is most easily carried out by using an analytical approximation to our calculated behavior of x_s . This approximation must be exceedingly accurate to allow the derivation of the other parameters. We have found that writing x_s in the form

$$x_s = x_s(0) \left\{ \frac{1 + c_1 W + c_2 W^2 + c_3 W^3}{1 + d_1 W + d_2 W^2 + d_3 W^3} \right\} \quad (29)$$

where the coefficients are as given in Table 3 and $W \equiv z^{7-3\omega}$ provides sufficient accuracy. Then $x_s^* = (7-3\omega)W(dx_s/dW)/x_s$ is straight-

forward. The postshock quantities then follow directly for any radius: $p_s(z) = p_s(R_1)z^{-3}$, $\rho_s(z) = x_s(z)\rho_0(R_1)z^{-\omega}$; v_s , F_s , and u_s follow from equation (1). The quantity $R_s \ell_s / F_s \approx x_s(2.53-\omega)$ can then be used in the two equations (3) to find α and β . Equation (13) is used to find η and v follows from the identity $\alpha-\beta = v+\eta$. Your algebra can be checked by comparing the results with those found from equation (7). This procedure supplies the postshock conditions and their derivatives at any value of z . The complete density structure is provided by equation (20). In order to find the remainder of the structure or the time evolution of an individual parcel, one performs numerical integrations as in Section II.

Suppose one wishes to learn the past history of a particular gas parcel now located at $r_f = R_f/R_s$. Equation (20) provides its current mass fraction μ_f and at any other epoch, $\mu = \mu_f(z_p/z)^{3-\omega}$. Thus the parcel was first encountered by the shock when $z = z_1 = z_p(\mu_f)^{1/(3-\omega)}$ when $\mu = \mu_1 = 1$. Conditions in the parcel at that moment are found as before since it is then the postshock gas. From these conditions one evaluates $K_1 = [x_s(z_1)]^{-5/2} z_1^{(5\omega-9)/2}$ and $C_1 = [1.1/1.2]^{3/2} K_1$.

From that point, one steps forward in z , following the time with equation (19) and the evolution of K and C with equations (21). At each new shock position z , one must calculate μ for the parcel, invert equation (20) to find r and then x (using the new postshock values of x_s and α), find $n = x n_0(R_1)z^{-\omega}$, calculate T and $g = T_e/T$ from C and K , calculate (if desired) p from n and T , calculate any desired ionization and recombination rates and derivatives of ionic concentrations, and finally calculate new derivatives of K and C from equations (22), (23), and (24) using the contemporary values of K , C ,

g , x , y , x' and μ for the parcel and of z , x_s , v at the shock. The procedure appears somewhat messy but it adds very little to the number of integrals which have to be performed anyway to follow the evolution of the ion concentrations.

IV. Discussion

The present work shows that including the effects of saturated thermal conduction depresses the shock compression factor x_s only modestly from the value of 4 appropriate to adiabatic calculations. We also find that the solution undergoes a sharp transition from the early time asymptote where thermal conduction dominates to the late asymptote where the structure is essentially adiabatic and the electron and ion temperatures are nearly equal over a large fraction of the remnant. The radius at which this occurs is quite similar to that given by Cowie (1977) for the equilibration of the two temperatures.

An error in the captions of Figures 2 and 3 of Paper I should be pointed out: actually the ambient density should be $\rho_0 \propto R_s^{+2}$ and $\rho_0 R_s^{+4}$ respectively.

This work was supported in part by NASA grant NGL 50-002-044 at the University of Wisconsin-Madison.

Table 1

Variables, Derivatives, and Normalizations

Variable	Symbol f	Postshock Derivative ($\partial \ln f / \partial \ln R$) _s	Normalized Form
radius	R		$r = R/R_s$
shock radius	R_s		$z = R_s/R_1$
time	t		$\tau = t/t_1$
density	ρ	$\alpha = (\partial \ln \rho / \partial \ln R)_s$	$x = \rho / \rho_0(R_s)$
nuclear number density	$n = \rho / (1.4 m_H / 1.1)$		
pressure	p	$\beta = (\partial \ln p / \partial \ln R)_s$	$y = p/p_s$
average temperature	T	$(\beta - \alpha) = (\partial \ln T / \partial \ln R)_s$	
electron temperature	T_e	$\eta = -(\partial \ln T_e / \partial \ln R)_s$	
mass velocity	u	$\sigma = (\partial \ln u / \partial \ln R)_s$	
shock velocity	v_s		
thermal conduction flux	F		
div F	ℓ		

Table 2

Solution Properties				
ω	z_{\max}^a	$x_s(0)$	$\epsilon(\omega)^b$	
			Early	Late
0	.858	3.2383	0.643	0.655
-2	.970	2.9121	0.578	0.581
-4	.998	2.7721	0.511	0.549

^athe value of z where x_s^* is maximum

^b $\epsilon(\omega) = E_0/[3V_{sp_s}/2]$; from Paper 1

Table 3

Analytical Fit Coefficients

ω	$x_s(0)$	c_1	c_2	c_3	d_1	d_2	d_3
0	3.2383	.37903	.069789	.014860	.32173	.059507	.012030
-2	2.9121	.50027	.11527	.040463	.38703	.091284	.029458
-4	2.7721	.54857	.13277	.054586	.40554	.10147	.037829

References

Cowie, L. L. and McKee, C. F. 1977, Ap. J., 211, 135.

Cowie, L. L. 1977, Ap. J., 215, 226.

Cox, D. P. and Anderson, P. R. 1982, Ap. J., 253, 268 (CA).

Cox, D. P. and Edgar, R. J. 1983, Ap. J., 265, 443 (Paper I).

Cox, D. P. and Franco, J. 1981, Ap. J., 251, 687 (CF).

Kahn, F. D. 1975, in Proc. Int. Cosmic Ray Conf., (Munich), 11, 3566.

Figure Captions

Fig. 1 - Values of edge parameters and derivatives plotted as functions of normalized shock radius $z=R_s/R_1$, for ambient densities $\rho_0 \propto R_s^{-\omega}$

- a) The compression factor $x_s \equiv \rho_s/\rho_0$
- b) $x_s^* \equiv \partial \ln x_s / \partial \ln R_s$
- c) The logarithmic postshock density derivative
 $\alpha \equiv (\partial \ln \rho / \partial \ln R)_s$
- d) The logarithmic postshock pressure derivative
 $\beta \equiv (\partial \ln p / \partial \ln R)_s$
- e) The logarithmic postshock electron temperature derivative
 $\eta \equiv -(\partial \ln T_e / \partial \ln R)_s$
- f) The logarithmic derivative of the electron-to-average temperature ratio $\nu \equiv [\partial \ln (T_e/T) / \partial \ln R]_s$

Fig. 2 - Normalized age of the remnant $\tau = t/t_1$ as a function of normalized shock radius $z = R_s/R_1$

- a) $\omega = 0$, a uniform ambient density
- b) $\rho_0 \propto R^2$
- c) $\rho_0 \propto R^4$

Fig. 3 - Snapshots of the internal remnant structure for $\rho_0 = \text{constant}$

- a) Pressure in units of $p_s(R_1)$
- b) Average temperature (solid lines) and electron temperature in units of $T_s(R_1)$

c) Density in units of $\rho_0(R_1)$. Also plotted are ambient density (lower line) and post-shock density (upper line).

Fig. 4 - Same as Figure 3 but with $\rho_0 \propto R_S^2$.

Fig. 5 - Same as Figure 3 but with $\rho_0 \propto R_S^4$.

Richard J. Edgar: Space Physics Laboratory, Department of Physics, University of Wisconsin-Madison, 1150 University Avenue, Madison, WI 53706.

Donald P. Cox: Department of Space Physics and Astronomy, Rice University, Houston, TX 77001.

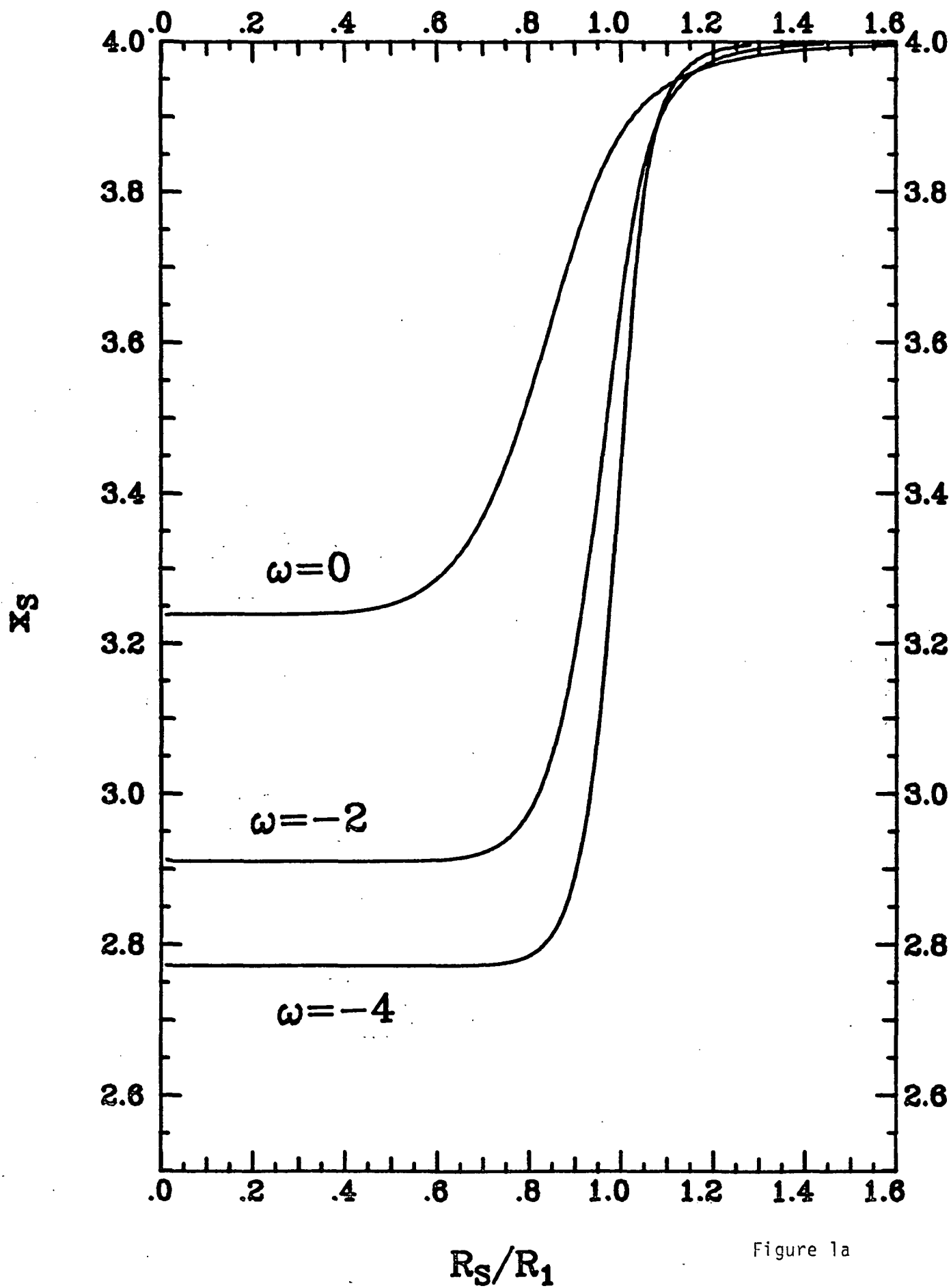


Figure 1a

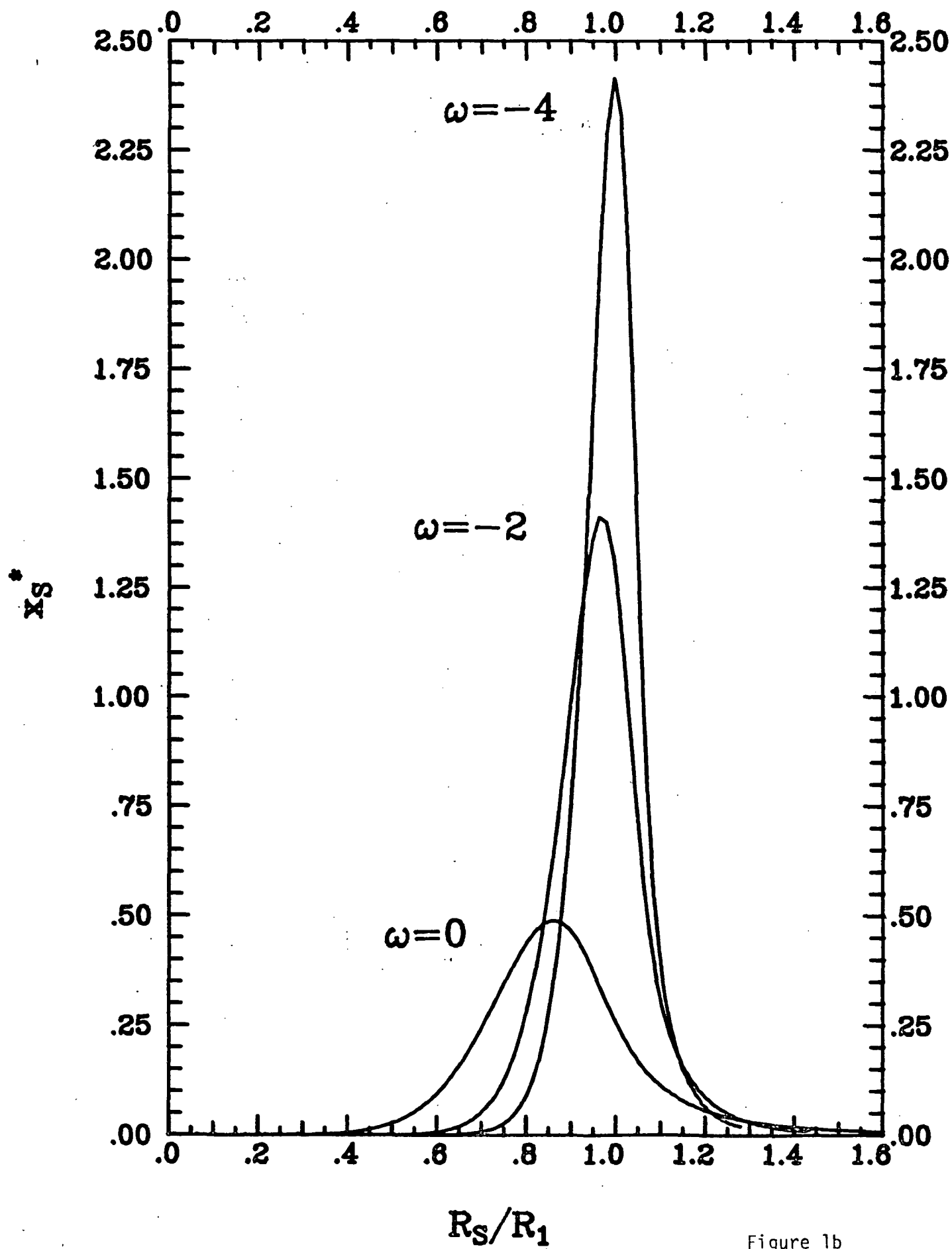


Figure 1b

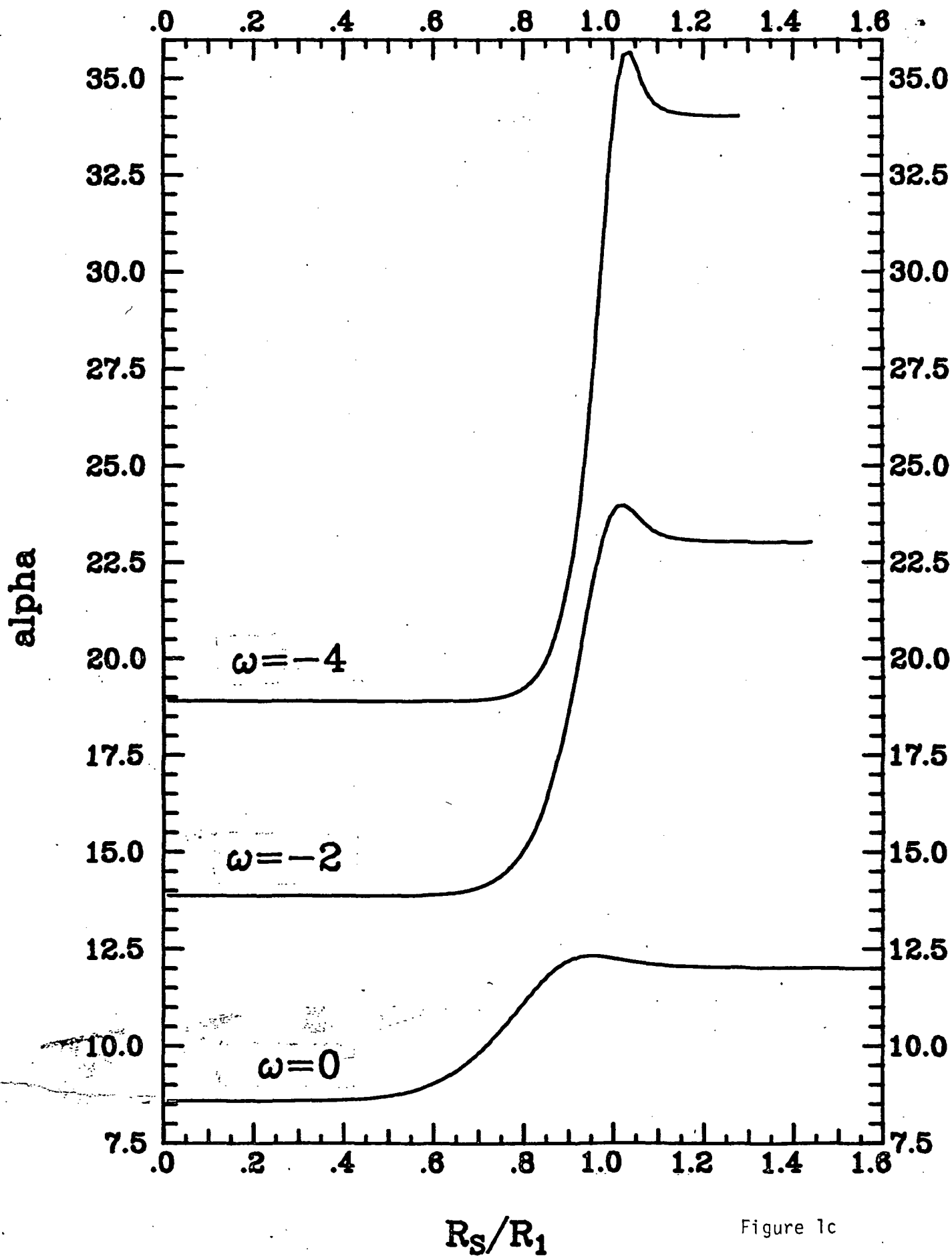


Figure 1c

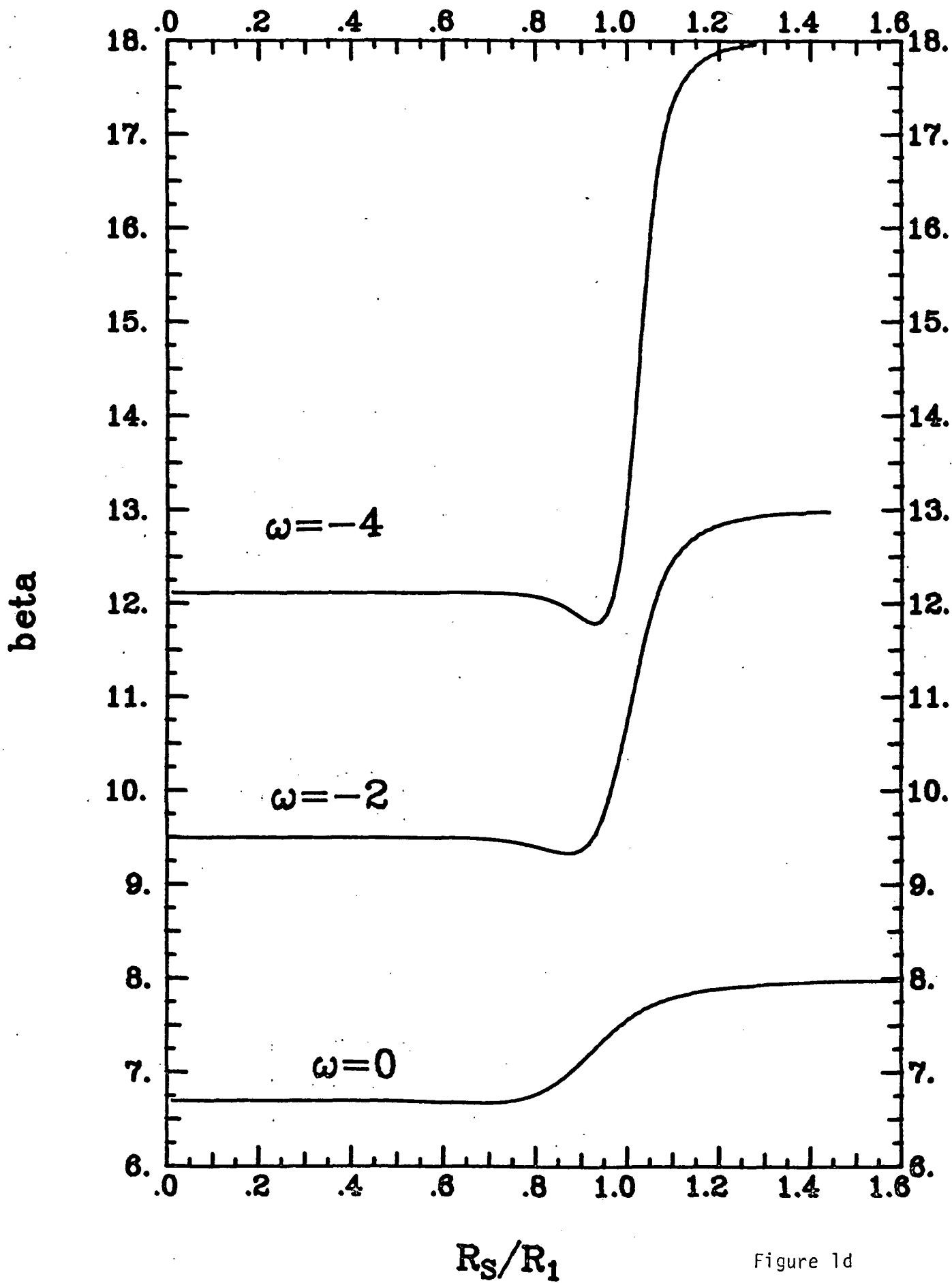


Figure 1d

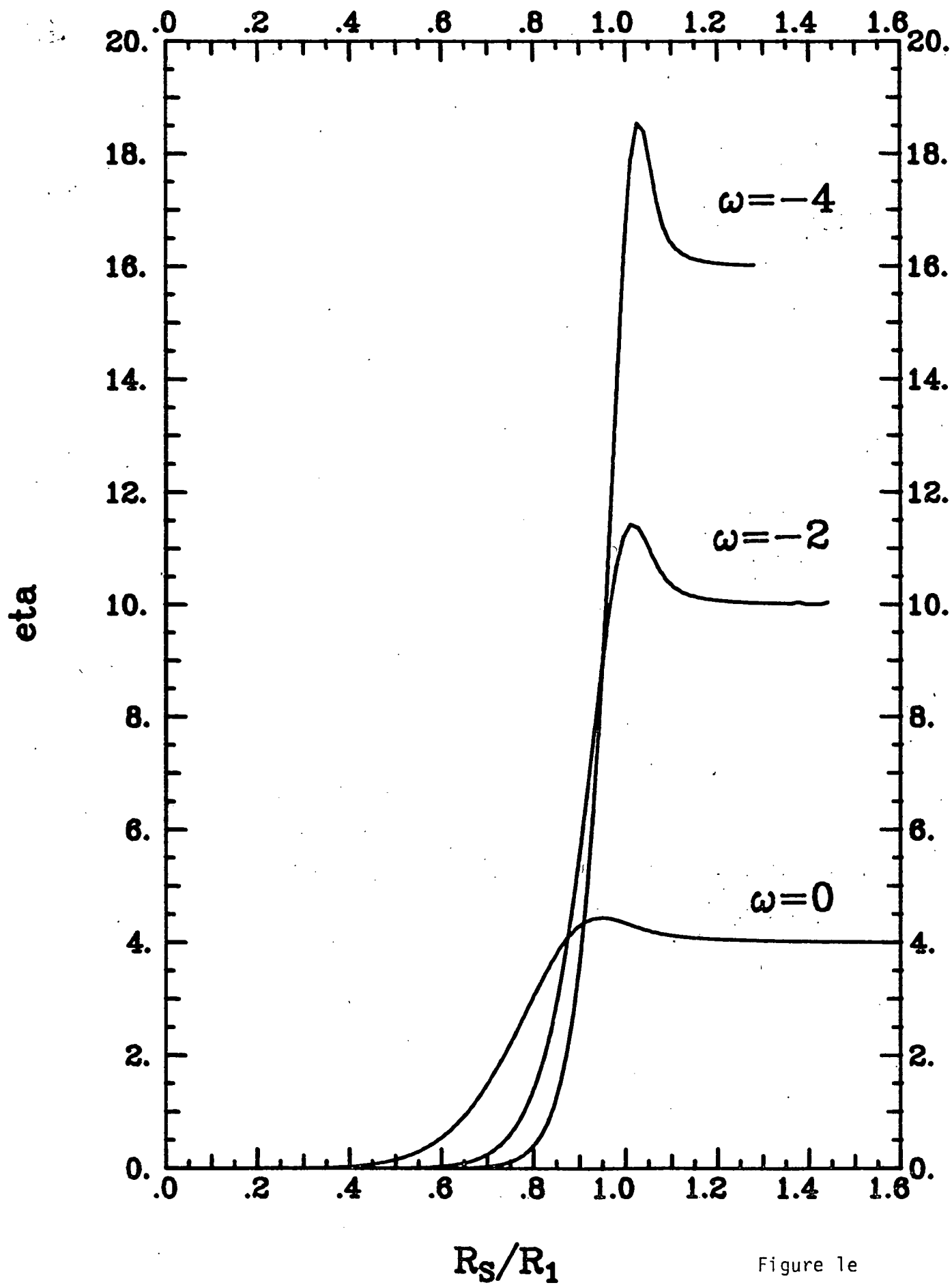


Figure 1e

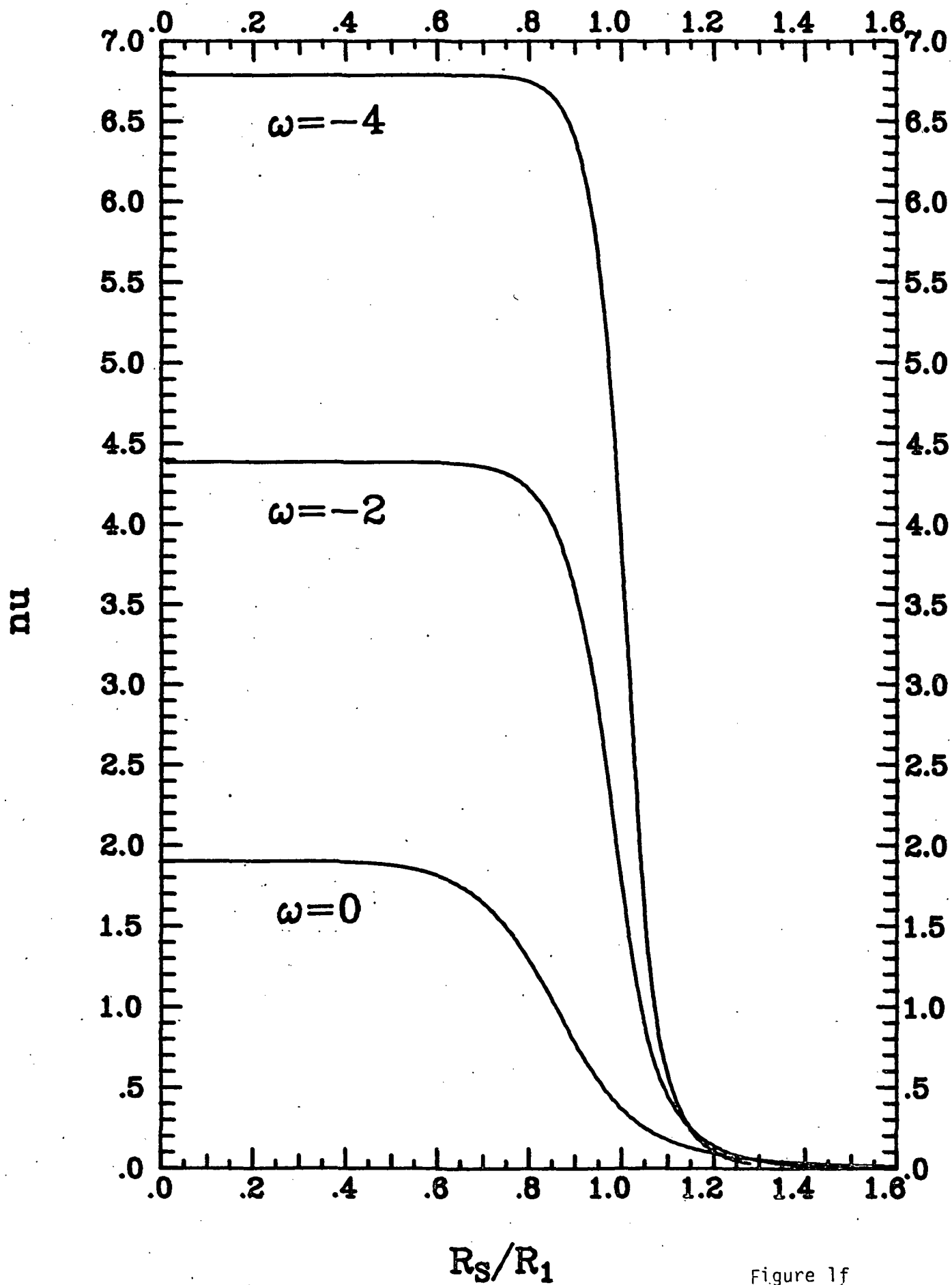


Figure 1f

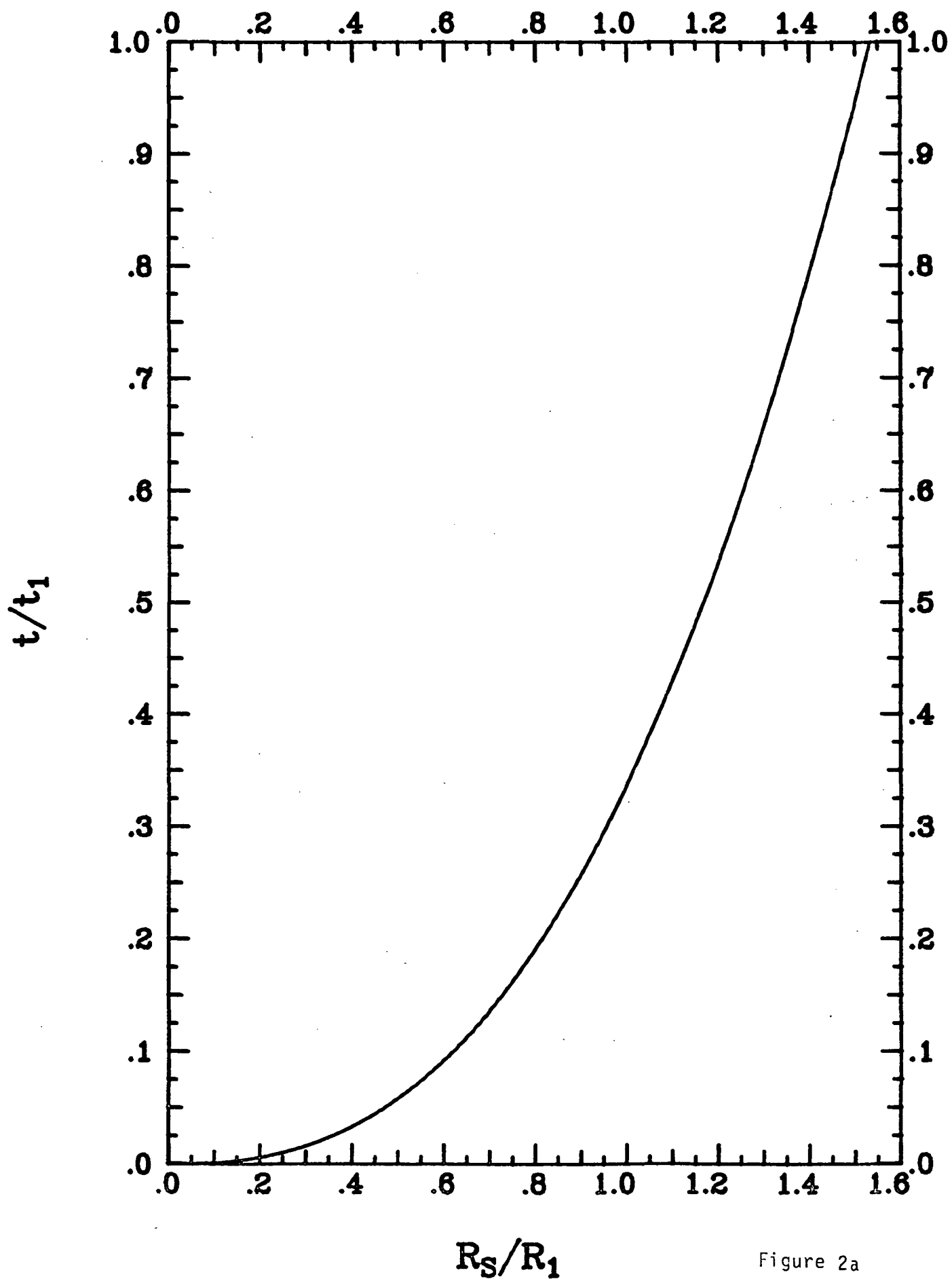


Figure 2a

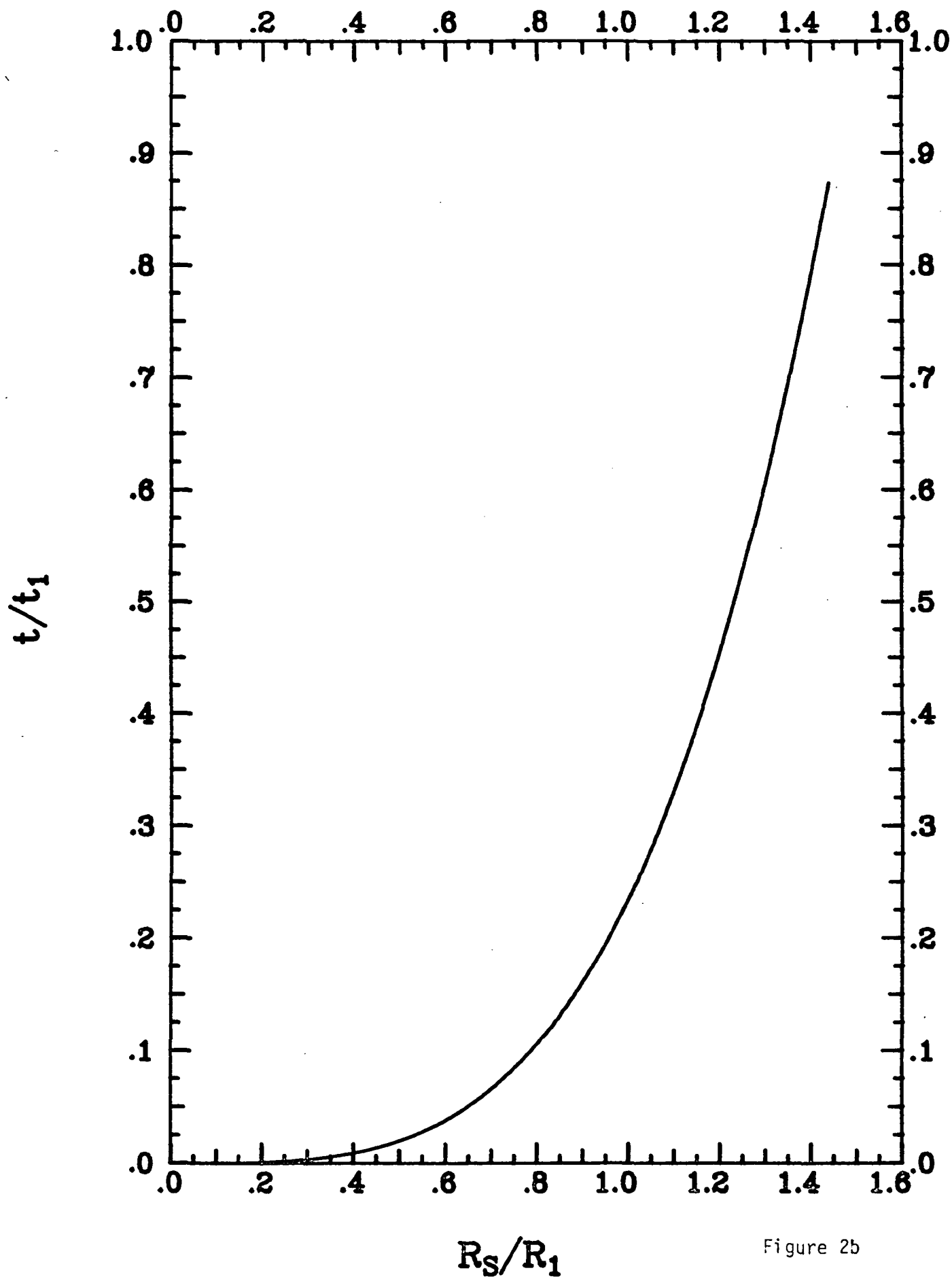


Figure 2b

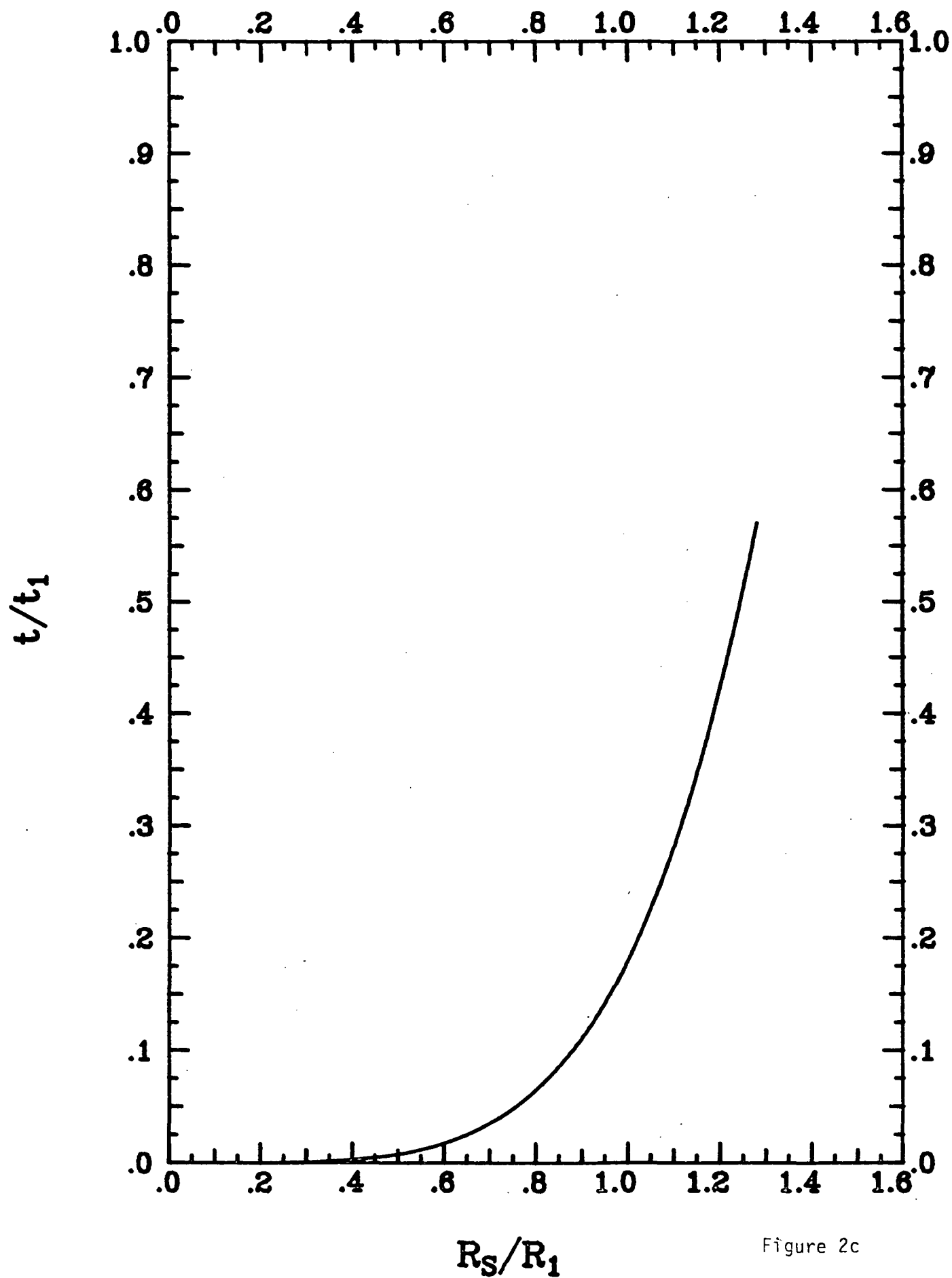


Figure 2c

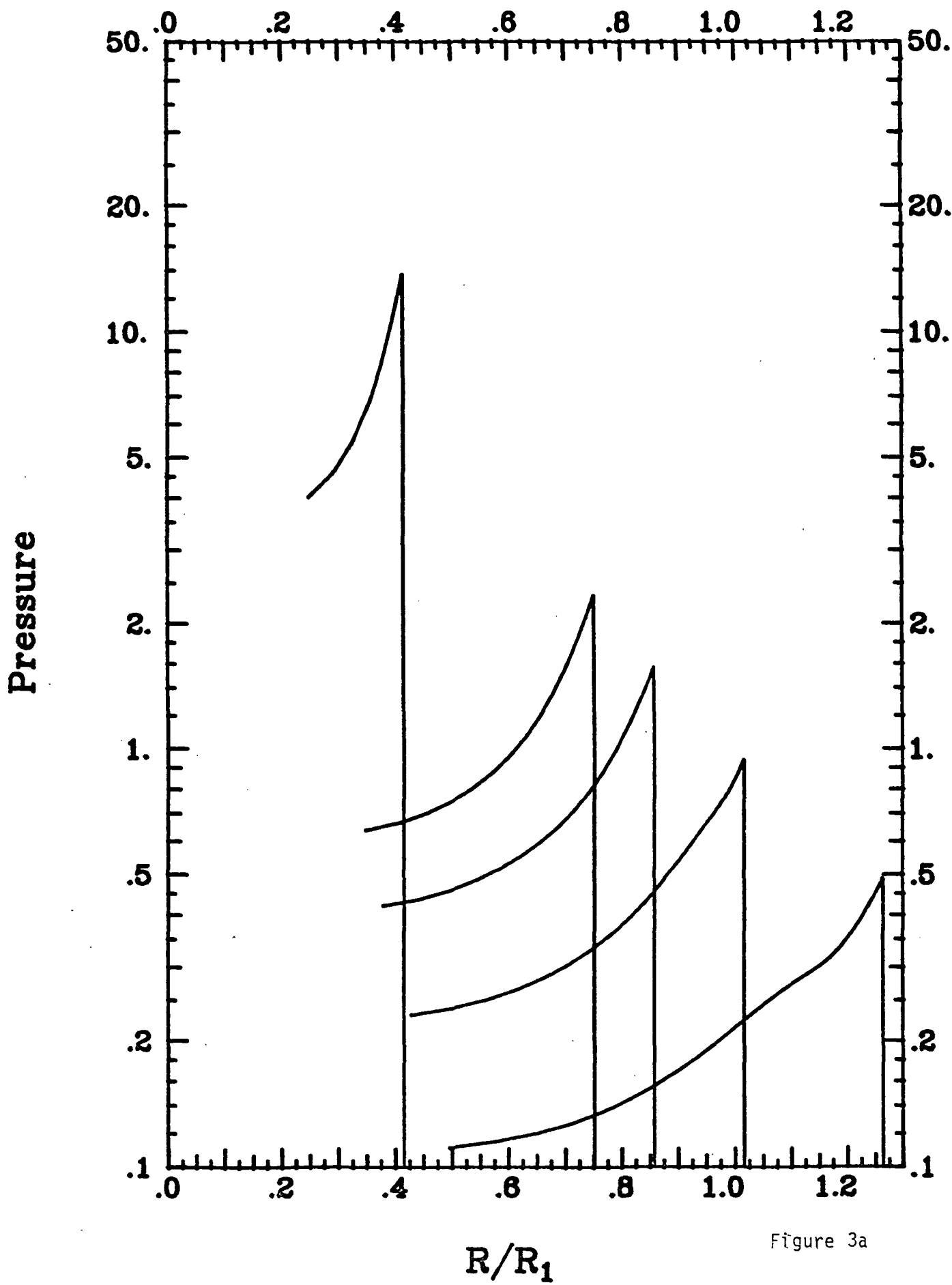


Figure 3a

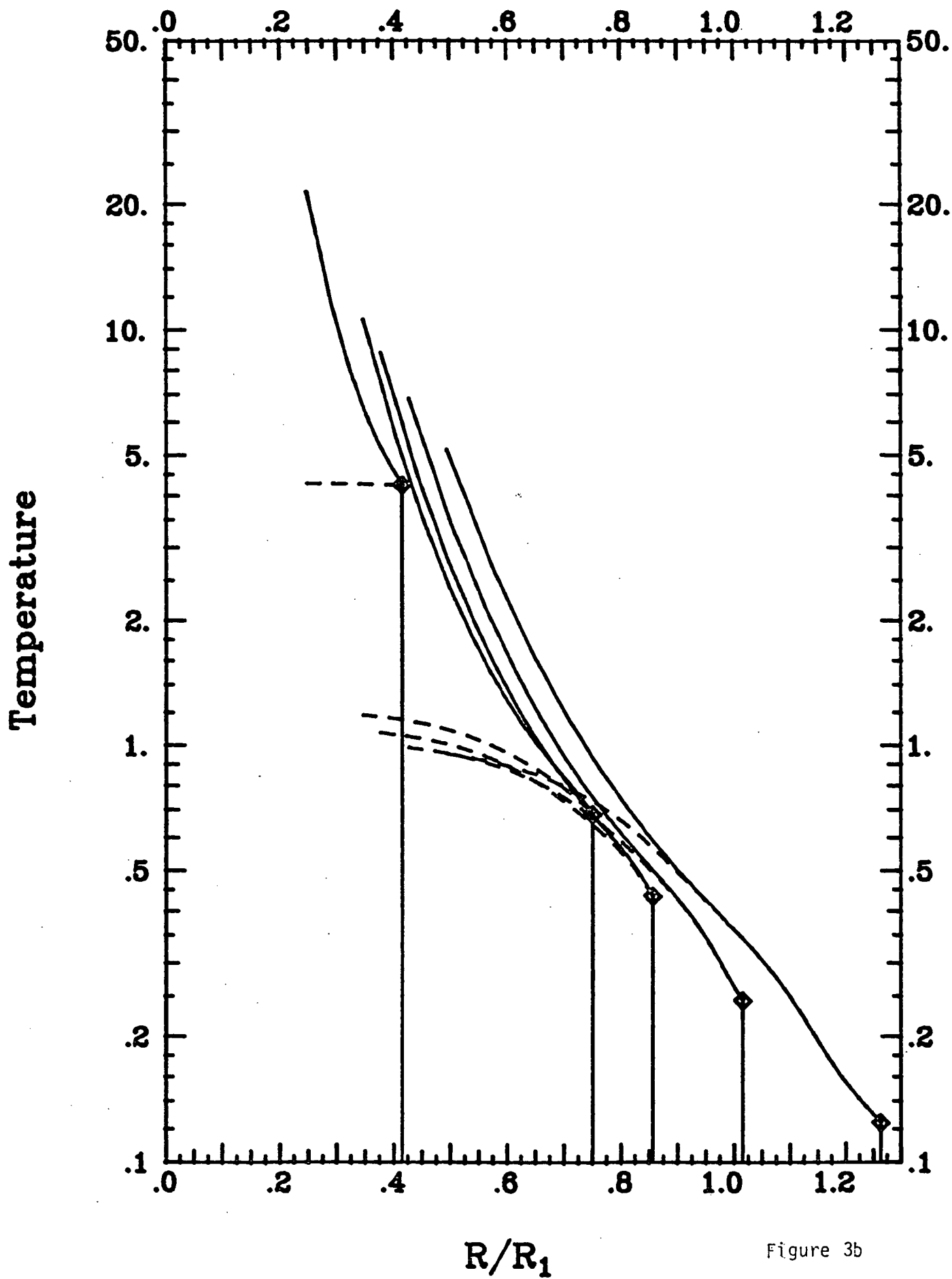


Figure 3b

Density

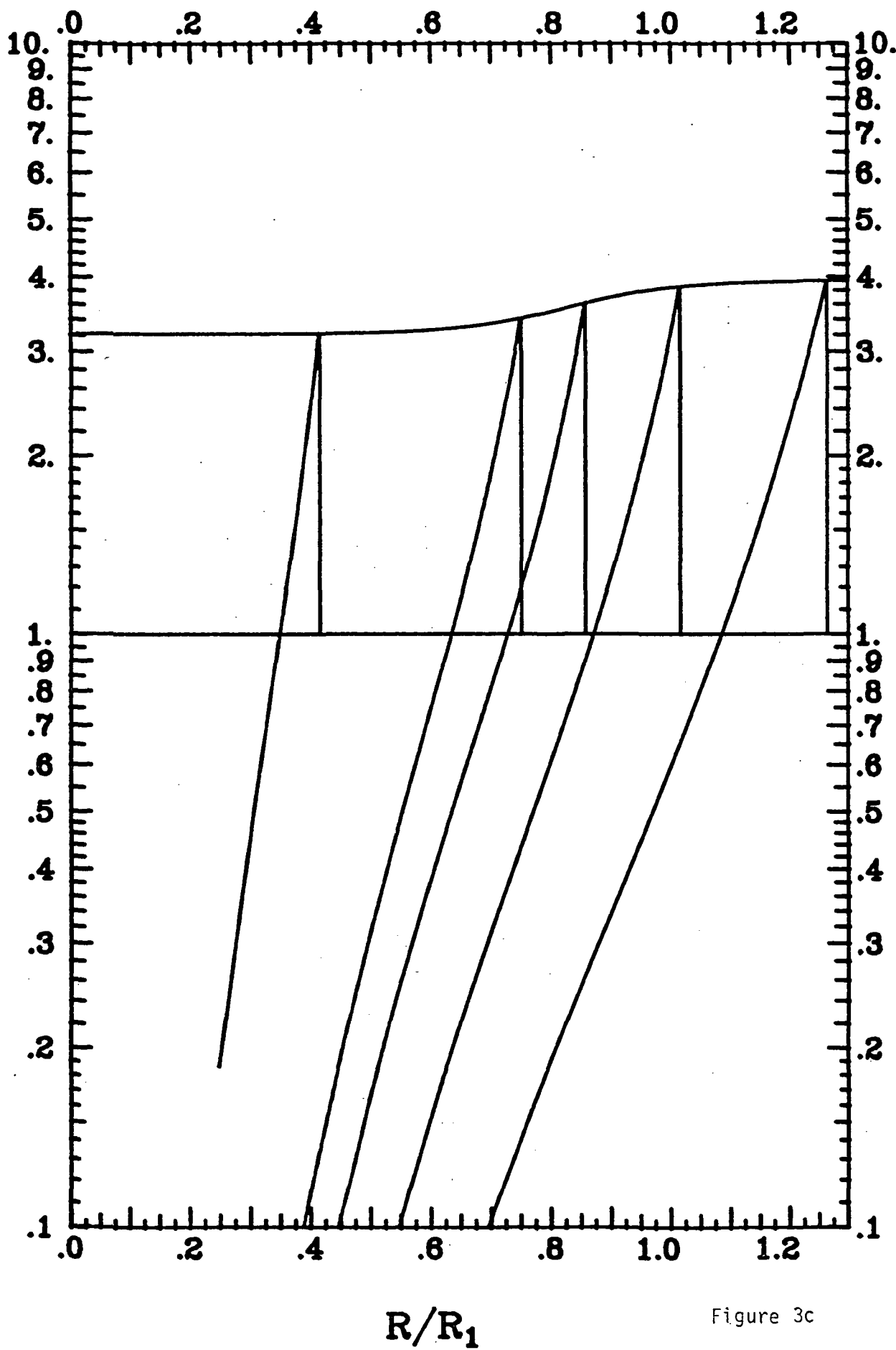


Figure 3c

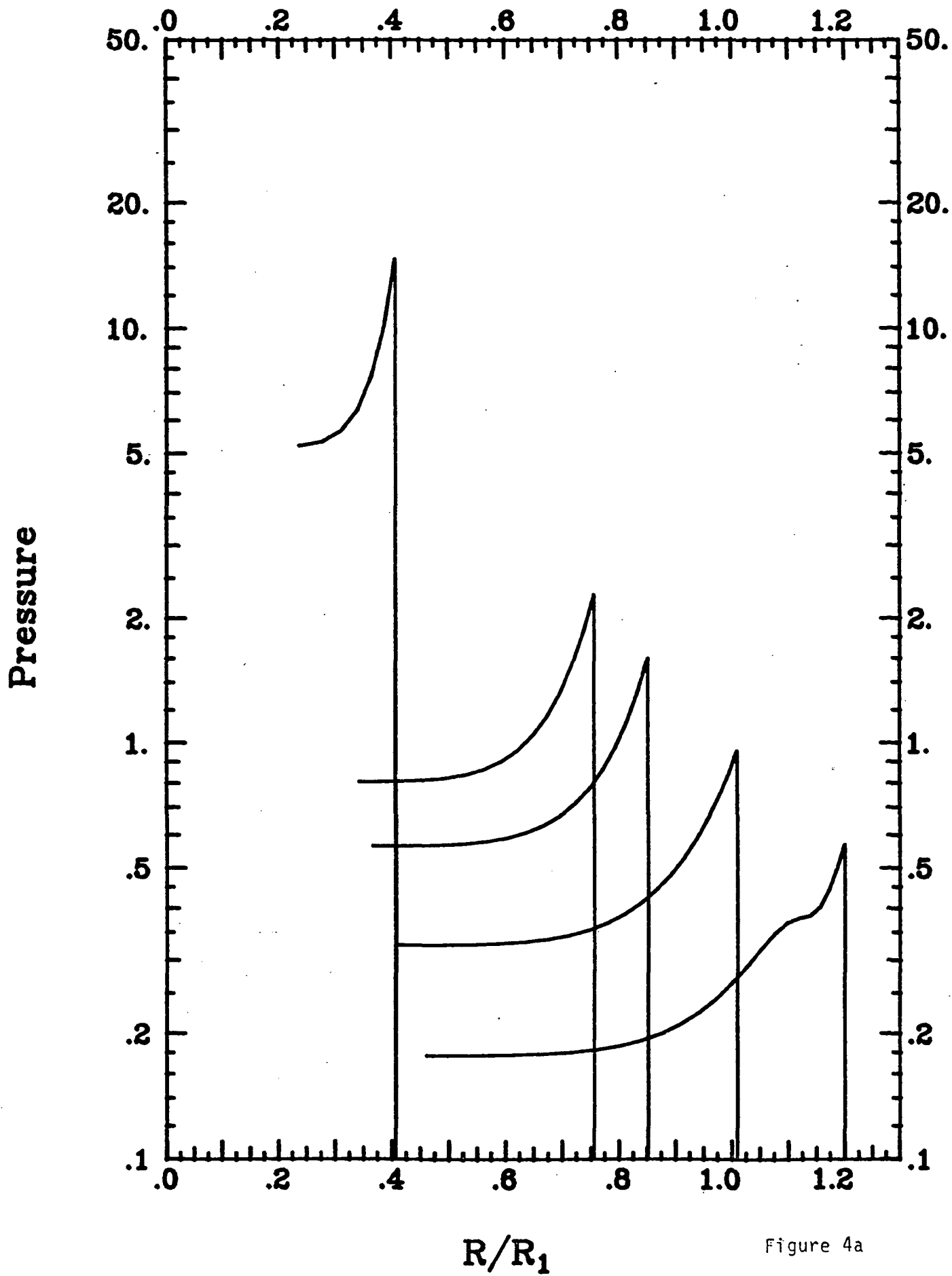


Figure 4a

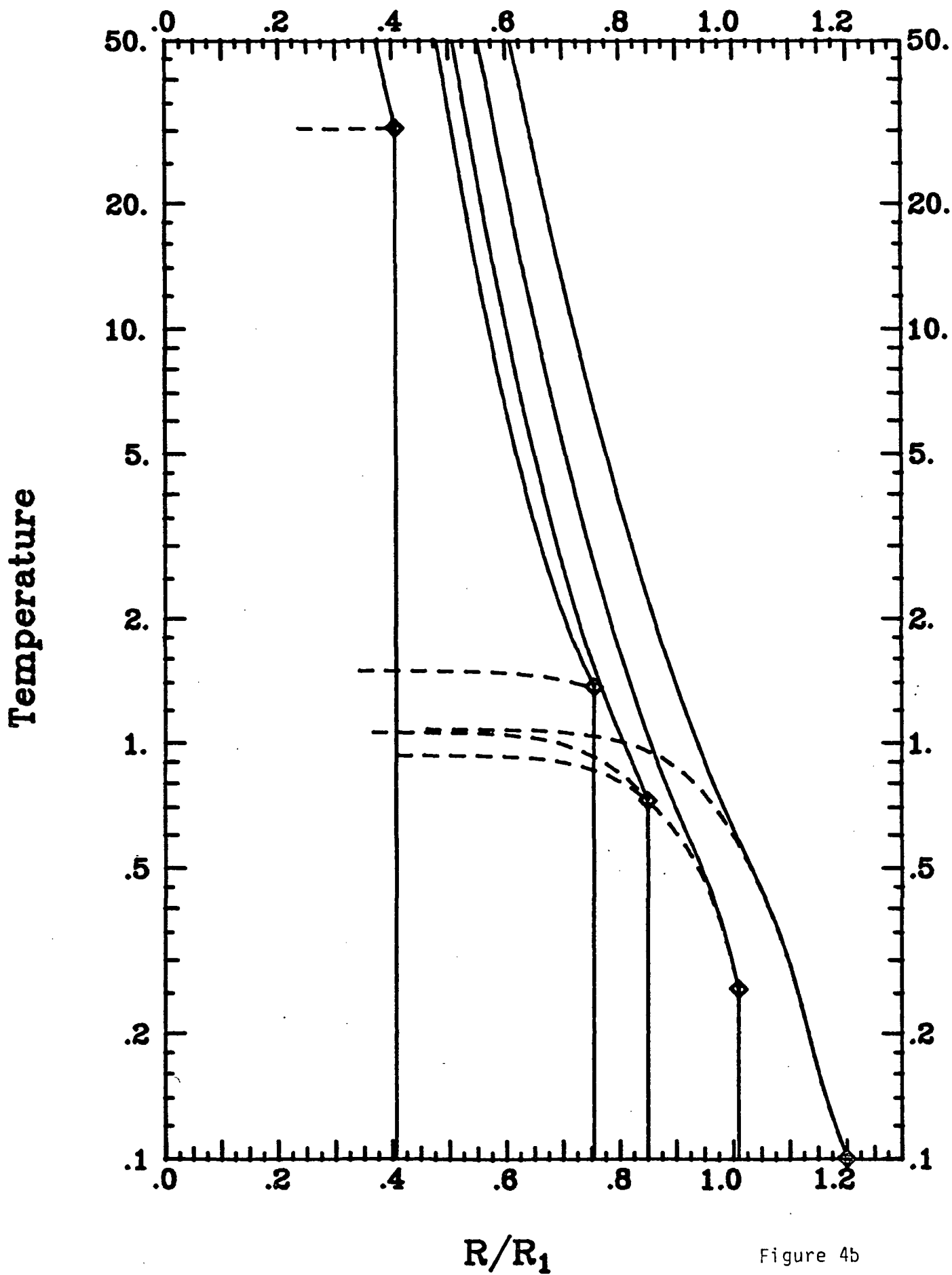


Figure 4b

Density

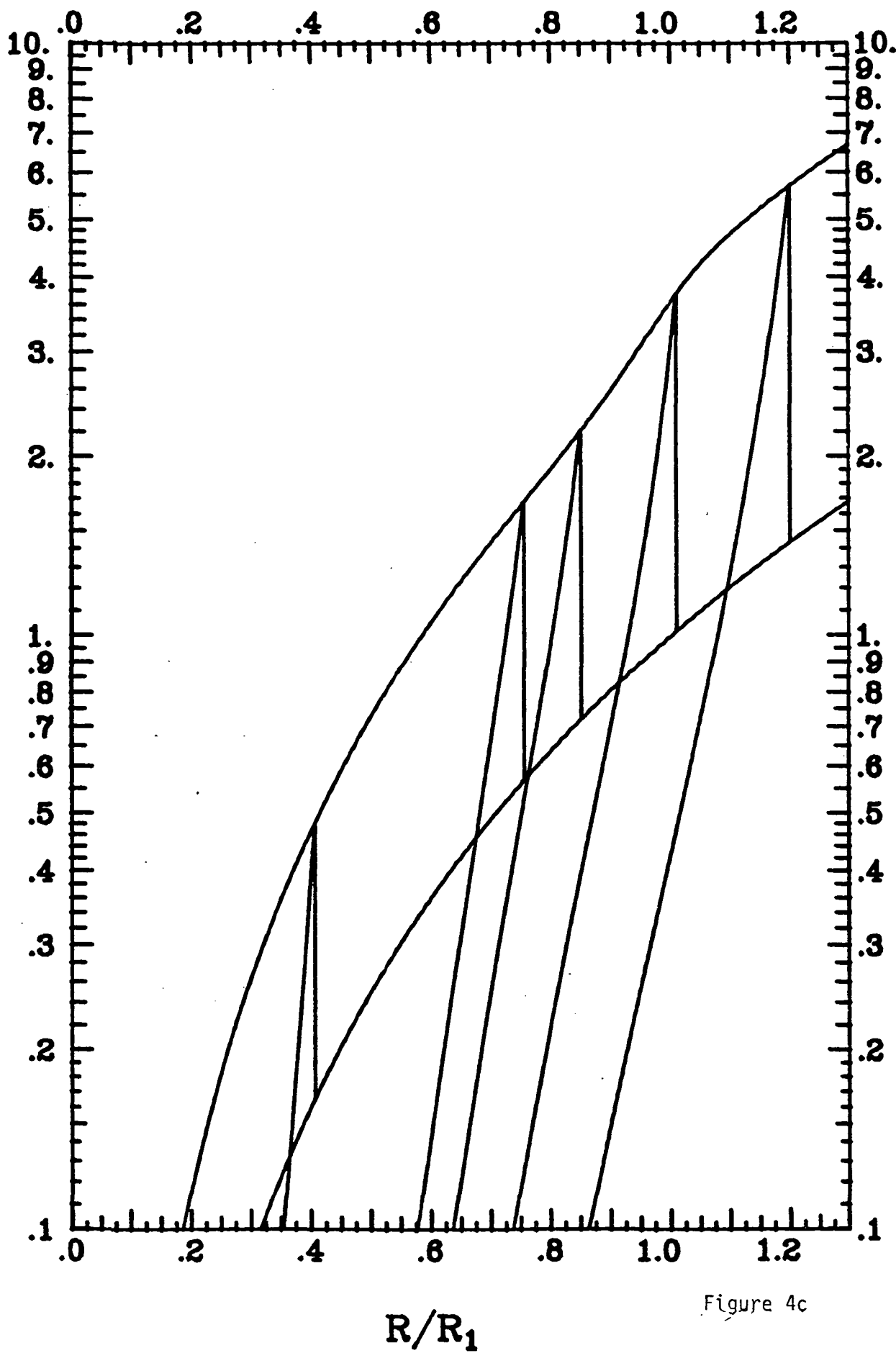


Figure 4c

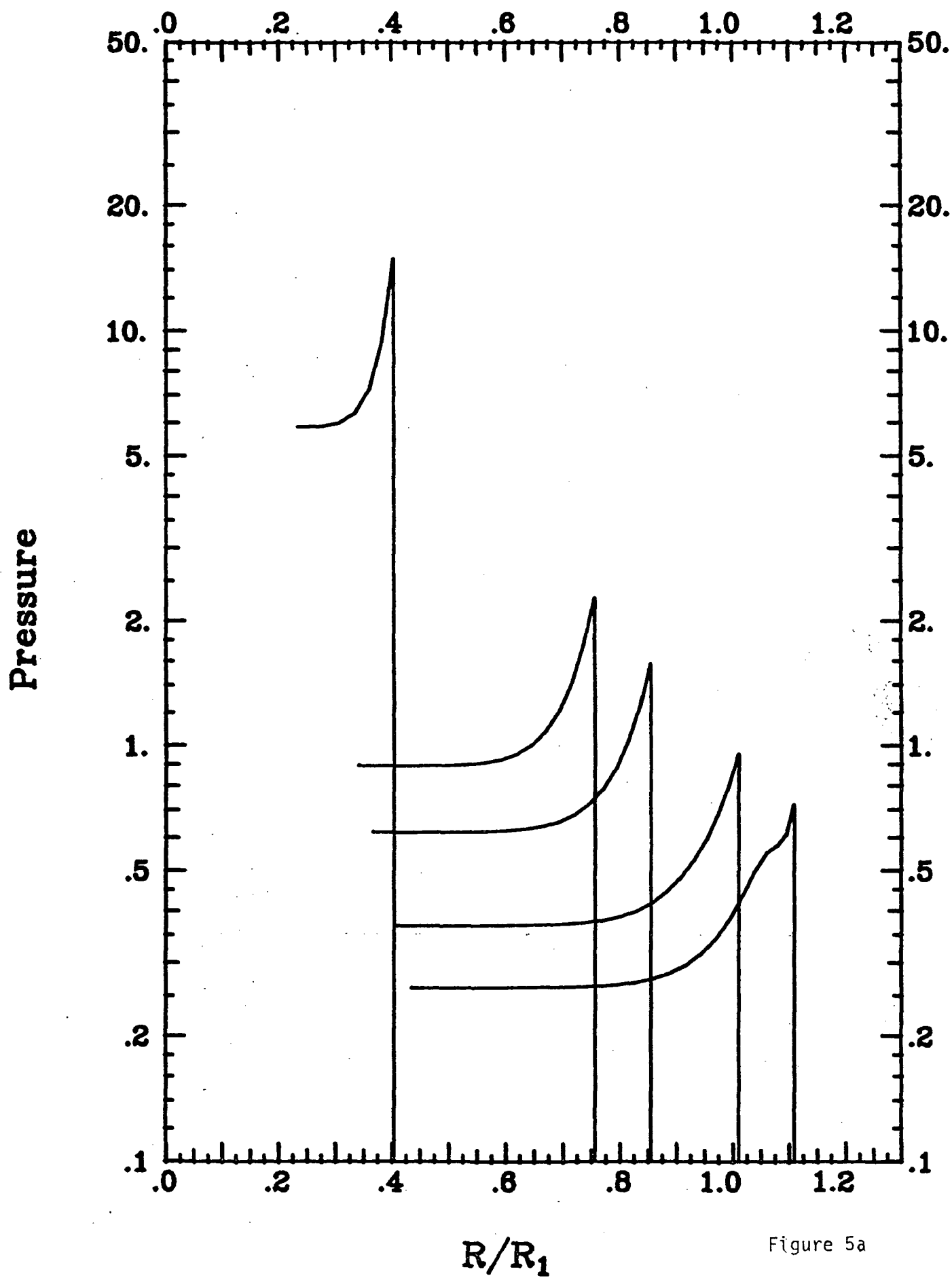


Figure 5a

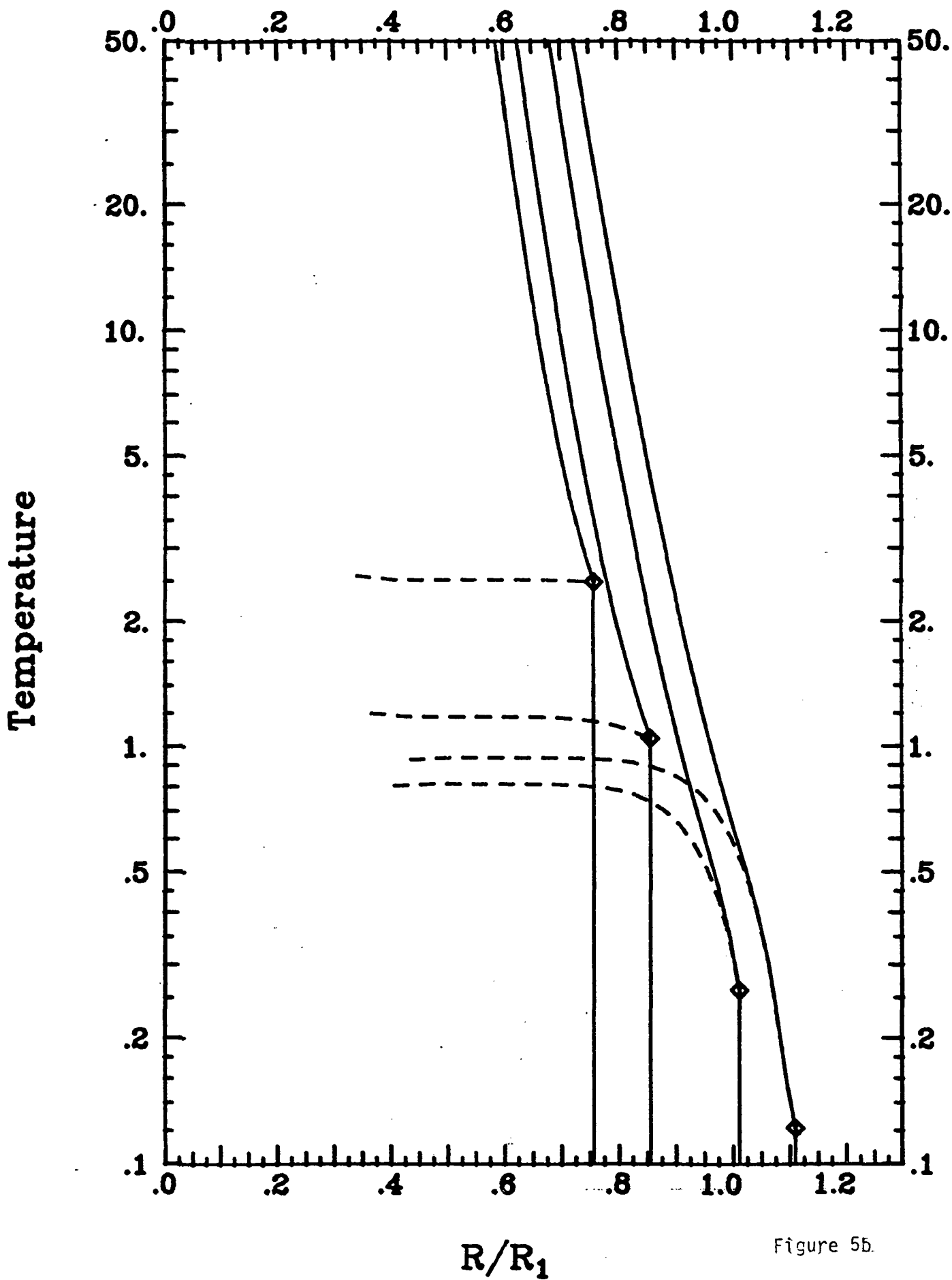
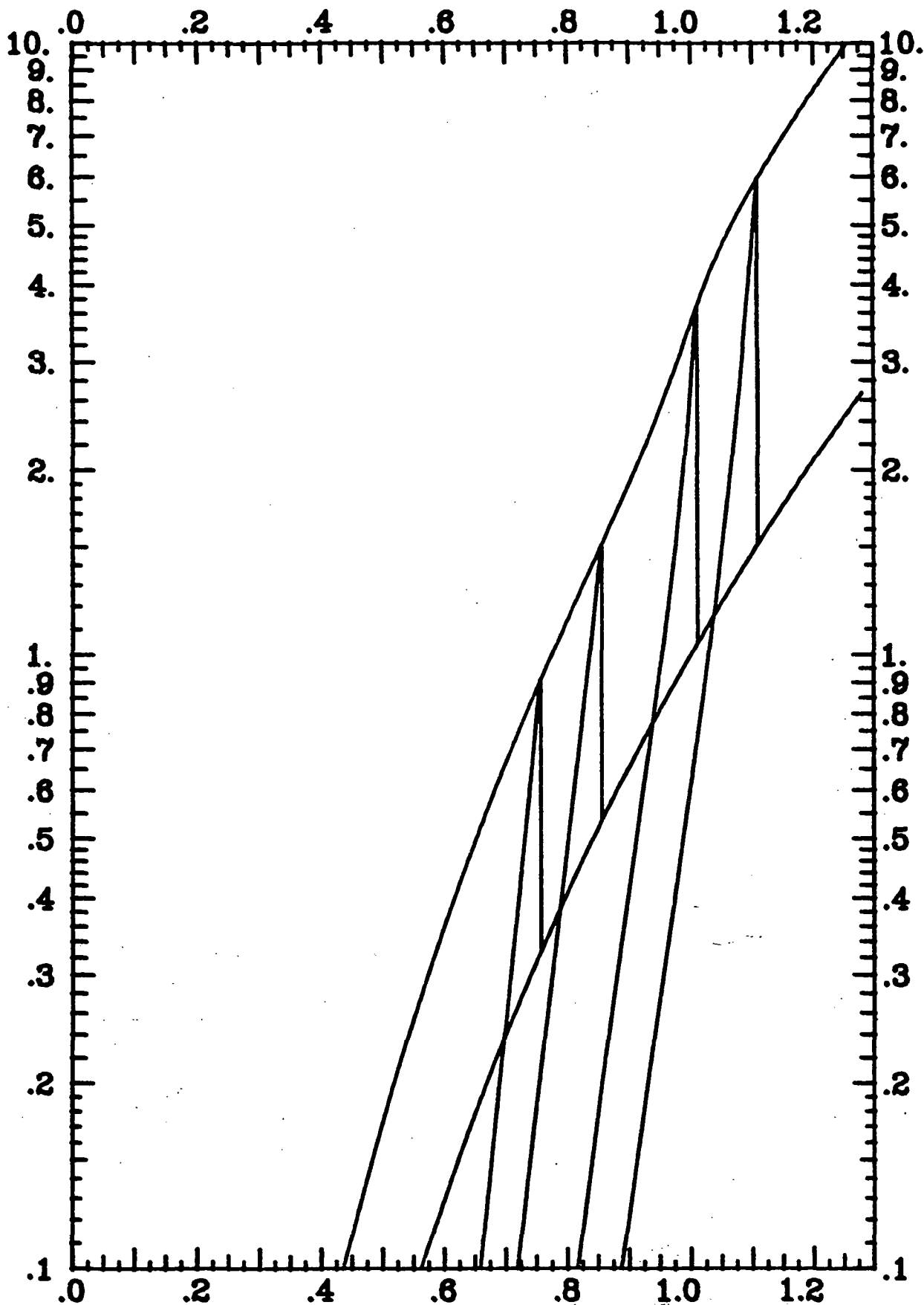


Figure 5b.

Density



R/R_1

Figure 5c